



Development of new carbon-11 labelled radiotracers for imaging GABA_A- and GABA_B-benzodiazepine receptors

Matthew D. Moran^a, Alan A. Wilson^a, Charles S. Elmore^{b,c}, Jun Parkes^a, Alvina Ng^a, Oleg Sadovski^a, Ariel Graff^a, Zafiris J. Daskalakis^a, Sylvain Houle^a, Marc J. Chapdelaine^b, Neil Vasdev^{a,*}

^a Centre for Addiction and Mental Health and University of Toronto, 250 College St., Toronto, ON, Canada M5T 1R8

^b Department of Chemistry, AstraZeneca Pharmaceuticals, Wilmington, DE 19850, United States

^c Department of DMPK, AstraZeneca Pharmaceuticals, Mölndal, Sweden

ARTICLE INFO

Article history:

Received 20 February 2012

Revised 5 May 2012

Accepted 12 May 2012

Available online 24 May 2012

Keywords:

Radiopharmaceuticals

Positron emission tomography

GABA_A receptors

GABA_B receptors

Carbon-11

ABSTRACT

Two quinolines identified as positive allosteric modulators of γ -aminobutyric acid (GABA)_A receptors containing the α_2 subunit, 9-amino-2-cyclobutyl-5-(6-methoxy-2-methylpyridin-3-yl)-2,3-dihydro-1H-pyrrolo[3,4-*b*]quinolin-1-one (**4**) and 9-amino-2-cyclobutyl-5-(2-methoxypyridin-3-yl)-2,3-dihydro-1H-pyrrolo[3,4-*b*]quinolin-1-one (**5**), were radiolabelled at the methoxy position with carbon-11 (half-life = 20.4 min). These quinolines represent a new class of potential radiotracers for imaging the benzodiazepine site of GABA_A receptors with positron emission tomography (PET). Both radiotracers were reliably isolated following reaction of their respective pyridinone/pyridinol tautomeric precursors with [¹¹C]CH₃I in clinically useful, formulated quantities (2.9% and 2.7% uncorrected radiochemical yield, respectively, relative to [¹¹C]CO₂) with high specific activities (>70 GBq μ mol⁻¹; >2 Ci μ mol⁻¹) and high radiochemical purities (>95%). The radiosyntheses reported herein represent rare examples of selectively isolating radiolabelled compounds bearing [¹¹C]2-methoxypyridine moieties. Although both radiotracers demonstrated promising imaging characteristics based on preliminary ex vivo biodistribution studies in conscious rodents, higher brain uptake was observed with [¹¹C]**5** and therefore this radiotracer was further evaluated. Carbon-11 labelled **5** readily penetrated the brain (>1 standard uptake value in cortical regions at 15 min post-injection of the radiotracer), had an appropriate regional brain distribution for GABA_A receptors that appeared to be reversible, and did not show any appreciable radiometabolites in rat brain homogenates up to 15 min post-injection. Preadministration of flumazenil (**1**, 10 mg kg⁻¹) or **5** (5 mg kg⁻¹) effectively blocked >50% of [¹¹C]**5** binding to the GABA_A receptor-rich regions, thereby suggesting that this radiotracer is worthy of further evaluation for imaging GABA_A receptors. Additionally (*R,S*)-*N*-(1-(3-chloro-4-methoxyphenyl)ethyl)-3,3-diphenylpropan-1-amine, **6**, an allosteric modulator of GABA_B receptors, was efficiently labelled in one step using [¹¹C]methyl iodide. Ex vivo biodistribution studies in conscious rats showed low brain uptake, therefore, efforts are underway to discover alternative radiotracers to image GABA_B. In conclusion, [¹¹C]**5** is worthy of further evaluation in higher species for imaging GABA_A receptors in the central nervous system.

Published by Elsevier Ltd.

1. Introduction

Gamma-aminobutyric acid (GABA) receptors constitute the largest population of inhibitory neurotransmitter receptors in the mammalian brain. The GABA_A receptor is a gated chloride-ion channel with a primary GABA binding site as well as multiple allosteric modulatory sites. When GABA, in conjunction with positive allosteric modulatory compounds (benzodiazepines, barbiturates,

neurosteroids, etc.), binds to GABA_A receptors, conformational changes increase the permeability of the central pore to chloride ions, resulting in chloride flux that hyperpolarizes the neuron.¹ Of all the allosteric sites known for GABA_A, the benzodiazepine (BZ) site has been the most studied. The GABA_A receptor has a pentameric structure that is composed of seven families of protein subunits: α_{1-6} , β_{1-4} , γ_{1-3} , δ , ϵ , π and ρ_{1-3} .^{2,3} The α subunit is of particular importance in determining the pharmacology of BZ-type drugs and alcohol.^{4,5} Benzodiazepines (and related drugs that bind to the BZ site) are amongst the most widely prescribed drugs in modern medicine: in addition to their anxiolytic, anticonvulsant and sedative effects, they are extensively used in the treatment of several illnesses of high socioeconomic burden including Alzheimer's Disease, schizophrenia, chronic alcohol dependency,

* Corresponding author. Tel.: +1 617 643 4736; fax: +1 617 726 6165.

E-mail address: vasdev.neil@mgh.harvard.edu (N. Vasdev).

[†] Present address: Department of Nuclear Medicine and Molecular Imaging, Massachusetts General Hospital and Harvard Medical School, Boston, MA 02114, United States.

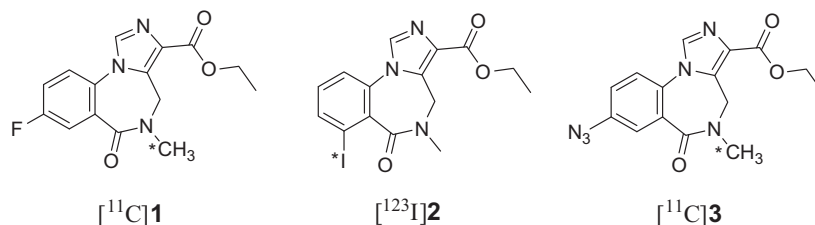


Figure 1. Commonly used radiotracers for imaging the BZ site of GABA_A.

mood disorders, post-traumatic stress disorder, etc., and are also postulated to play a role in cognition, consciousness and sleep.⁶ Further research has shown that subtype-selective compounds for the benzodiazepine site can have anti-anxiolytic effects while avoiding the side effects experienced from earlier BZs:^{7,8} including ataxia, sedation, potentiation of alcohol, tolerance and dependence upon chronic administration.^{9,10}

Positron emission tomography (PET) has been extensively used to image GABA_A receptors, and radiopharmaceutical development for this target has been extensively reviewed.⁶ The most well characterized radiopharmaceutical for imaging GABA_A receptors is $[^{11}\text{C}]\text{flumazenil}$ ($[^{11}\text{C}]\mathbf{1}$, Ro 15-1788, Fig. 1), a potent, non-subtype selective BZ inverse agonist that binds to the $\alpha_{1,2,3}$, and α_5 subunits on the BZ site on GABA_A receptors in the human brain.^{8,11,12} Derivatives of flumazenil have been labelled with carbon-11 at the ester moiety¹³ and with fluorine-18 at the 4-position of the phenyl ring^{14,15} and evaluated as PET radiopharmaceuticals in human subjects. The structurally related radioiodinated analogue, $[^{123}\text{I}]\text{iomazenil}$ ($[^{123}\text{I}]\mathbf{2}$, Ro 16-0154, Fig. 1) has been extensively used for single photon emission computed tomography (SPECT),¹⁶ and has alternately been radiolabelled with carbon-11 at the nitrogen atom (Fig. 1).¹⁷ Carbon-11 labelled $[^{11}\text{C}]\text{Ro15 4513}$ ($[^{11}\text{C}]\mathbf{3}$, Fig. 1) is an established radiotracer for GABA_A receptors in human subjects,^{18,19} and has more recently been proposed to be selective for the α_5 subtype.^{19,20} Other PET radiotracers for imaging GABA_A receptors include $[^{18}\text{F}]\text{fluoroethylflumazenil}$,^{21,22} $[^{11}\text{C}]\text{suriclone}$,²³ $[^{11}\text{C}]\text{flunitrazepam}$,²⁴ $[^{11}\text{C}]\text{diazepam}$,^{24,25} $[^{11}\text{C}]\text{fludiazepam}$,²⁶ and $[^{18}\text{F}]\text{oxoquazepam}$,²⁷ but these radiotracers all lack subtype selectivity. There is still a paucity of radiotracers developed for imaging the GABA_A receptor that are not derived from the BZ core.⁶

We here report the radiosyntheses of $[^{11}\text{C}]\text{9-amino-2-cyclobutyl-5-(6-methoxy-2-methylpyridin-3-yl)-2,3-dihydro-1H-pyrrolo[3,4-b]quinolin-1-one}$ ($[^{11}\text{C}]\mathbf{4}$)²⁸ and $[^{11}\text{C}]\text{9-amino-2-cyclobutyl-5-(2-methoxypyridin-3-yl)-2,3-dihydro-1H-pyrrolo[3,4-b]quinolin-1-one}$ ($[^{11}\text{C}]\mathbf{5}$) and biological evaluations of these non-benzodiazepine radiotracers in conscious rodent models with the goal of discovering improved PET radiotracers for imaging the BZ site of GABA_A. Compounds **4** and **5** were identified as having excellent potential for radiopharmaceutical development for the following reasons: (1) they are amenable for radiolabelling with carbon-11 at the methoxy position; (2) recently reported structure-activity relationship studies have identified that these quinolines are potent towards the GABA_A α_1 and α_2 -subunits but selective over α_5 -subunits;²⁸ and (3) these functionally selective compounds would represent a potentially new class of quinoline-based radiotracers for imaging the BZ site of GABA_A receptors.^{28,29} Both radiotracers were evaluated ex vivo in rat brain regions and whole blood, and where appropriate, metabolite analyses were conducted on both brain homogenates and plasma.

While GABA_A receptors have been extensively studied with PET,⁶ there are currently no radiotracers for imaging GABA_B receptors in the living human brain. The GABA_B receptors are considered an important target in the brain, as they have been implicated in addiction to alcohol^{30,31} and cocaine,³² as well as epilepsy.³³ Radiotracer leads for this elusive target are still sparse, with only two

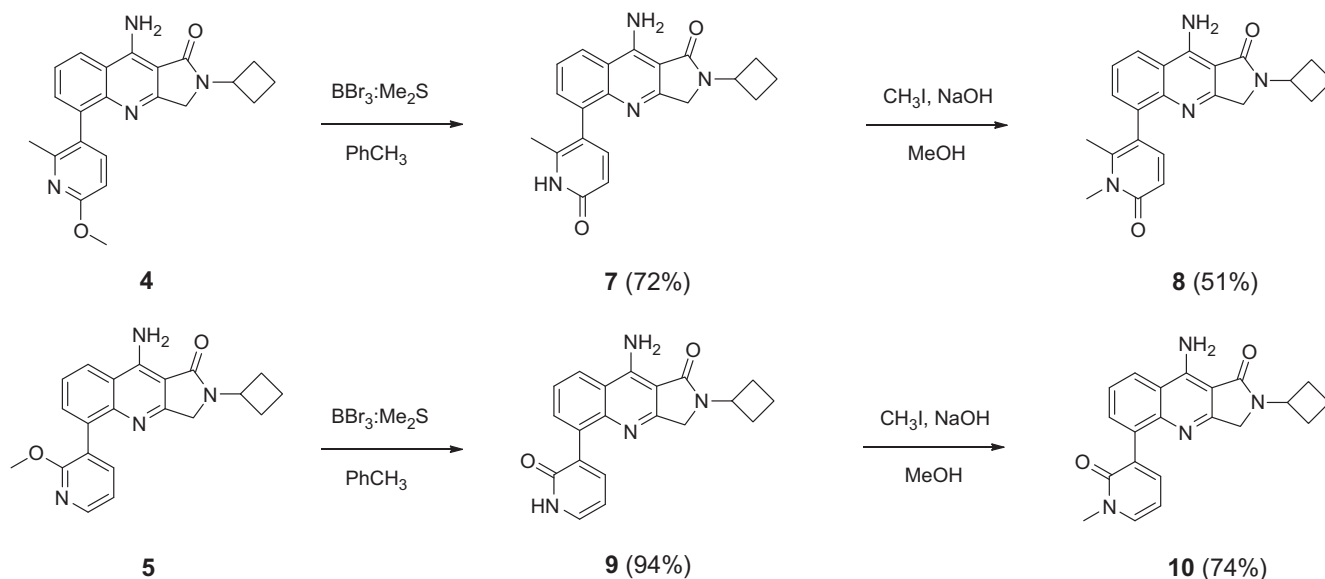
reported attempts to develop radiolabelled compounds for imaging GABA_B receptors: CGP62349, a GABA_B receptor antagonist, was successfully labelled with carbon-11 (^{11}C ; $t_{1/2} = 20.4$ min) but did not penetrate rat brain,²³ while $[^{11}\text{C}]\text{-baclofen}$, a radiotracer based on a GABA_B receptor agonist, has not been evaluated in vivo.³⁴ Kerr and co-workers have identified a number of fendiline derivatives that are potent positive allosteric modulators for the GABA_B receptor, with (*R,S*)-*N*-(1-(3-chloro-4-methoxyphenyl)ethyl)-3,3-diphenylpropan-1-amine (**6**) displaying high potency for this target (EC_{50} , 10 nM).³⁵ Herein we also report the radiosynthesis of carbon-11 labelled (*R,S*)-*N*-(1-(3-chloro-4-methoxyphenyl)ethyl)-3,3-diphenylpropan-1-amine ($[^{11}\text{C}]\mathbf{6}$) as a potential radiotracer for imaging GABA_B receptors, and preliminary ex vivo brain biodistribution studies following tail-vein injection of this radiotracer in conscious rats.

2. Results

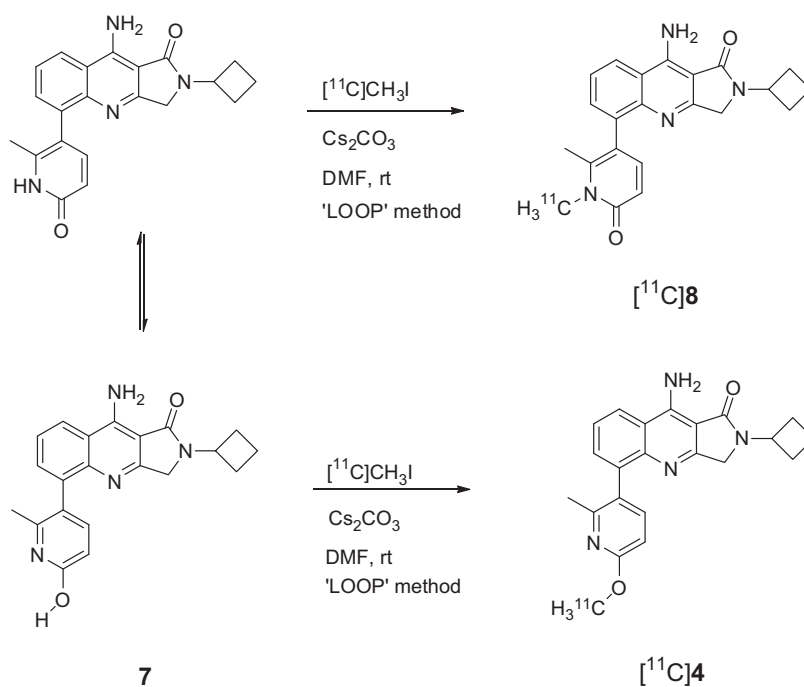
2.1. Chemistry and radiochemistry

Our radiosynthetic strategy for the preparation of $[^{11}\text{C}]\mathbf{4}$ and $[^{11}\text{C}]\mathbf{5}$, involves reaction of their respective desmethyl precursors with $[^{11}\text{C}]\text{CH}_3\text{I}$. Both 9-amino-2-cyclobutyl-5-(2-methyl-6-oxo-1,6-dihydropyridin-3-yl)-2,3-dihydro-1H-pyrrolo[3,4-b]quinolin-1-one (**7**) and 9-amino-2-cyclobutyl-5-(2-oxo-1,2-dihydropyridin-3-yl)-2,3-dihydro-1H-pyrrolo[3,4-b]quinolin-1-one (**9**), were efficiently prepared by demethylation of **4** and **5**, respectively (Scheme 1). Because compounds **7** and **9** exist as tautomers between their pyridinone and pyridinol forms (Schemes 2 and 3), reactions with $[^{11}\text{C}]\text{CH}_3\text{I}$ will most likely favor the methylation reaction at the secondary amine of this moiety (vide infra). Therefore, 9-amino-2-cyclobutyl-5-(1,2-dimethyl-6-oxo-1,6-dihydropyridin-3-yl)-2,3-dihydro-1H-pyrrolo[3,4-b]quinolin-1-one (**8**) and 9-amino-2-cyclobutyl-5-(1-methyl-2-oxo-1,2-dihydropyridin-3-yl)-2,3-dihydro-1H-pyrrolo[3,4-b]quinolin-1-one (**10**), were prepared by reaction of methyl iodide in the presence of base, with **7** or **9**, respectively (Scheme 1), to serve as reference standards during radiochromatographic separation and analyses.

Preparation of $[^{11}\text{C}]\mathbf{4}$ and $[^{11}\text{C}]\mathbf{5}$ were successfully accomplished by reactions of $[^{11}\text{C}]\text{CH}_3\text{I}$ with **7** and **9**, respectively (Schemes 2 and 3). While previous work has demonstrated that methylation reactions using silver carbonate as the base most favors formation of the desired methylated oxygen product with similar structural motifs,^{36,37} analogous reactions failed to yield the products in our hands. Instead, Cs_2CO_3 was found to give the best conversions (Table S1) and was utilized as the base to achieve reasonable conversions to $[^{11}\text{C}]\mathbf{4}$ and $[^{11}\text{C}]\mathbf{5}$ at room temperature. As anticipated, the major radiochemical products, $[^{11}\text{C}]\mathbf{8}$ and $[^{11}\text{C}]\mathbf{10}$, were identified by coinjection with authentic **8** and **10**, respectively, and were effectively separated post-synthesis by HPLC (ratio of $[^{11}\text{C}]\mathbf{4}:[^{11}\text{C}]\mathbf{8} \approx [^{11}\text{C}]\mathbf{5}:[^{11}\text{C}]\mathbf{10} \approx 1:4$). The radiosyntheses reported herein represent rare examples of selectively isolating $[^{11}\text{C}]$ -2-methoxypyridine moieties and should prove to be generally applicable within this class of compounds.



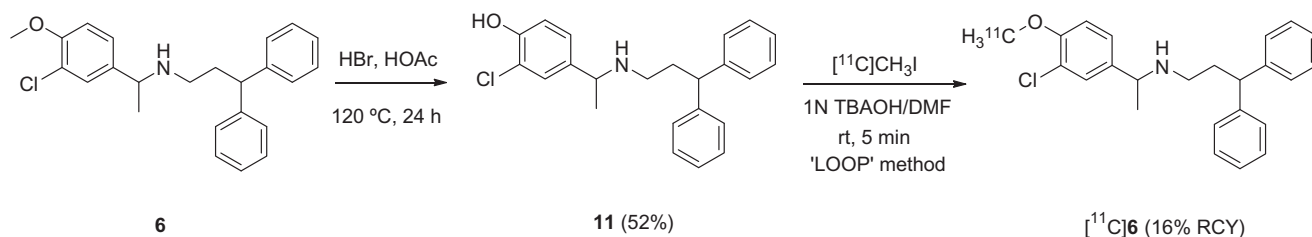
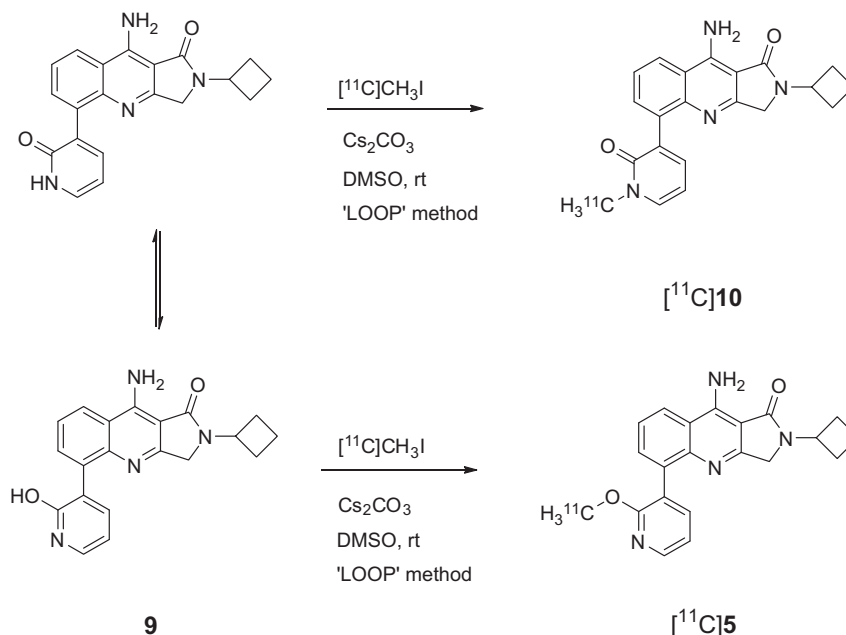
Scheme 1. Preparation of compounds 7–10.

Scheme 2. Preparation of [^{11}C]4 and the undesired product, [^{11}C]8.

Automated reactions of **7** (DMF, 25 °C, 1 min, Scheme 2) and **9** (DMSO, 25 °C, 1 min, Scheme 3) with [^{11}C]methyl iodide were accomplished in a clean, dry HPLC loop (the 'LOOP' method)³⁸ using a modified radiofluorination module.³⁹ After purification by HPLC (Figs. S1a and S2a) and formulation, the products, [^{11}C]4 and [^{11}C]5, were obtained in 2.9% (910.6 MBq, 24.6 mCi) and 2.7% (847.8 MBq, 23.0 mCi) radiochemical yields, respectively (based on our full scale production of [^{11}C]CO₂ (31.4 GBq; 850 mCi) uncorrected for decay). The times to end-of-synthesis (EOS) were 30 min, with the formulated products having specific activities of $100 \pm 30 \text{ GBq } \mu\text{mol}^{-1}$ ($2.7 \pm 0.9 \text{ Ci } \mu\text{mol}^{-1}$; $n = 6$) and $70 \pm 20 \text{ GBq } \mu\text{mol}^{-1}$ ($2.0 \pm 0.5 \text{ Ci } \mu\text{mol}^{-1}$; $n = 6$), respectively, with radiochemical purities >95% (Figs. S1b and S2b). Co-injection of the radioactive products with authentic standards of **4** and **5** under

different conditions (solvents, pH), with different analytical columns, further established the identity of the radiotracers. Under all conditions [^{11}C]4 and [^{11}C]5 co-chromatographed with authentic **4** and **5**. On storage for 120 min, both compounds did not show signs of radiolysis as determined by HPLC analysis.

Compound **6**³⁵ was *O*-demethylated in moderate yield to prepare the desmethyl precursor, **11** (Scheme 4). Clinically useful quantities of [^{11}C]6 (5.0 GBq, 136 mCi) were efficiently achieved by reactions of **11** with [^{11}C]CH₃I (Scheme 4) in DMF in the presence of tetrabutylammonium hydroxide (1 N TBAOH in MeOH) via the 'LOOP' method³⁸ using a modified GE TRACERlabTM FX_{FN} radiosynthesis module.³⁹ After purification by preparative HPLC (Fig. S3) and formulation, [^{11}C]6 was obtained in a radiochemical yield (RCY) of 16% (uncorrected for decay, based on production of



31.4 GBq (850 mCi) of [^{11}C]CO₂), in a synthesis time of 30 min. Analysis of the final formulated product by HPLC (Fig. S4) gave a specific activity of 160 ± 40 GBq μmol^{-1} (4.3 ± 1.2 Ci μmol^{-1} ; $n = 3$), and a radiochemical purity >99% at end of synthesis.

2.2. Ex vivo biodistribution studies with [^{11}C]5 in rats

Preliminary biodistribution studies of [^{11}C]4 and [^{11}C]5 (Fig. S5) and [^{11}C]6 (Table S2) were carried out as previously described by our group,⁴⁰ and demonstrated that [^{11}C]5 had higher uptake in rat brain than [^{11}C]4; as such, this compound was chosen for further evaluations for imaging GABA_A. Upon tail-vein injection of [^{11}C]6, however, only low levels of radioactivity (<0.2% injected dose per gram of wet tissue (%ID/g) across all brain regions at all time points) were taken up in rat brain (Table S2). Because successful radiotracers for imaging the central nervous system (CNS) typically express a %ID/g of tissue $\geq 0.5\%$ in rat brain,⁴¹ the relatively low brain uptake of [^{11}C]6 precluded its further study for imaging central GABA_B in vivo.

While physicochemical properties of a potential PET radiotracer for imaging neuroreceptors has not been well determined, log *P* values (lipophilicities) between 2 and 3 are considered ideal.⁴² At physiological pH (7.40), using the octanol/buffer shake-flask method,⁴³ the log *D*_{7.4} of [^{11}C]4 was 4.12 ± 0.06 ($n = 8$), while the log *D*_{7.4} of [^{11}C]5 was 3.00 ± 0.06 . The log *D*_{7.4} of [^{11}C]6 was 3.2 ± 0.1 . Our future efforts are aimed at developing less lipophilic fendiline derivatives as potential therapeutics and radiotracers for imaging GABA_B receptors.

Upon tail-vein injection of [^{11}C]5, moderate levels of radioactivity (>0.4% ID/g) were taken up in rat brain at early time points (Table 1, $n = 4$ per time point), and were effectively cleared by 60 min post injection. The regional heterogeneity of radioactivity reflects the known distribution of GABA_A in rat brain,⁴⁴ with the highest levels of radioactivity in the frontal cortex and rest of cortex. The fast kinetics of uptake and washout of radioactivity is also a favorable characteristic for a potential radiotracer labelled with carbon-11.

2.3. Metabolism studies

The presence of significant quantities of radioactive metabolites in the regions of interest during a PET scan may confound measurements (i.e. improper quantification of the images and interpretation of the results).⁴⁵ In order to quantify the extent of

Table 1
Ex vivo biodistribution of [^{11}C]5 in rodents (%ID/g (decay-corrected), $n = 4$).

	Time (post injection)			
	5 min	15 min	30 min	60 min
Cerebellum	0.36 ± 0.02	0.34 ± 0.05	0.26 ± 0.05	0.13 ± 0.02
Hippocampus	0.20 ± 0.06	0.29 ± 0.05	0.24 ± 0.04	0.09 ± 0.02
Striatum	0.26 ± 0.02	0.21 ± 0.04	0.15 ± 0.06	0.06 ± 0.01
Cortex (front)	0.47 ± 0.07	0.53 ± 0.08	0.44 ± 0.09	0.21 ± 0.05
Cortex (rest)	0.45 ± 0.03	0.46 ± 0.06	0.37 ± 0.06	0.16 ± 0.02
Rest	0.25 ± 0.02	0.27 ± 0.04	0.22 ± 0.05	0.11 ± 0.02
Blood	0.14 ± 0.1	0.15 ± 0.04	0.11 ± 0.03	0.08 ± 0.01

metabolism of [^{11}C]5, rats ($n = 2$ per time point) were injected with the radiotracer (tail-vein), and homogenized brain extracts and plasma were isolated at 5 and 15 min post injection. While the HPLC analysis of radioactivity in rat plasma at 15 min post injection showed significant metabolism to both a hydrophilic ($t_R = 1$ min) and a lipophilic ($t_R = 5.3$ min) metabolite (71% parent compound at 15 min post injection, Fig. 2b; showing the rapid metabolism at 5 min), no radioactive metabolites were detected in the brain, with [^{11}C]5 accounting for >99% of the radioactivity present in the rat brain tissue at 15 min post injection (Fig. 2a). Thus, the metabolites present in the plasma are not reflected in brain tissue and unlikely to interfere with imaging studies of central nervous system (CNS) GABA_A receptors.

2.4. Blocking studies

In light of the promising biodistribution and metabolism studies, blocking studies were carried out with [^{11}C]5. Four groups of rats were pretreated (i.p.) at 30 min prior to administration of [^{11}C]5 with: (1) vehicle (5% DMSO/5% EtOH in saline containing 5% Tween80 w/w), (2) 0.1 mg/kg of **5**, (3) 5 mg/kg of **5**, and (4) 10 mg/kg of **1** (highly selective for the α_1 , α_2 , α_3 , and α_5 subunits). All groups were sacrificed at 15 min post injection of the radiotracer (Table 2).

Specificity of binding to GABA_A was demonstrated by showing >70% reduction of radioactivity in brain regions of interest, including cerebellum, hippocampus and cortical regions, by treatment with high doses of **5** (5 mg/kg) and **1** (10 mg/kg; Table 2). These findings indicate that [^{11}C]5 likely binds selectively to GABA_A in the rat brain.

3. Conclusion

The present work has demonstrated that [^{11}C]4, [^{11}C]5 and [^{11}C]6 can be reliably synthesized in quantities and at the specific activities and radiochemical purities required for human PET studies, and the radiolabelling of a pyridinone/pyridinol tautomeric precursor developed herein should be broadly applicable to the preparation of structurally related [^{11}C]2-methoxypyridine moieties with [^{11}C]CH₃I. Furthermore, [^{11}C]6 represents a rare example of a radiotracer developed for imaging GABA_B receptors that has been evaluated in vivo. While [^{11}C]6 was not readily taken up in rat brain, the ex vivo biodistribution studies of [^{11}C]5 demonstrate that this radiotracer readily crosses the blood-brain barrier, has an appropriate regional brain distribution for GABA_A receptors, and

Table 2

Effect of drug pretreatment on the specific binding of [^{11}C]5 in rat brain (%ID/g).

	Treatment (dose, mg/kg)			
	Vehicle	5 (0.1)	5 (5.0)	1 (10)
Cerebellum	0.26 ± 0.02	0.22 ± 0.04	0.12 ± 0.03	0.09 ± 0.03
Hippocampus	0.22 ± 0.02	0.17 ± 0.04	0.11 ± 0.02	0.08 ± 0.03
Striatum	0.13 ± 0.02	0.14 ± 0.01	0.10 ± 0.01	0.08 ± 0.02
Cortex (front)	0.42 ± 0.04	0.36 ± 0.07	0.16 ± 0.06	0.13 ± 0.06
Cortex (rest)	0.36 ± 0.02	0.27 ± 0.11	0.14 ± 0.05	0.11 ± 0.04
Rest	0.20 ± 0.01	0.16 ± 0.07	0.09 ± 0.04	0.09 ± 0.02
Blood	0.11 ± 0.01	0.11 ± 0.01	0.12 ± 0.01	0.12 ± 0.01

displays binding that appeared to be reversible. The ex vivo pharmacology is indicative of selective binding to GABA_A receptors, as pre-administration of flumazenil or **5** blocks specific uptake of the radiotracer. Plasma and brain radioactive metabolite measurements are in full accord with the desired properties of a selective GABA_A receptor imaging agent for PET. The above-mentioned properties indicate that [^{11}C]5 and related quinoline derivatives are leading-candidate radiotracers worthy of further exploration for imaging GABA_A receptors in higher species.

4. Experimental section

4.1. General methods

The compounds 9-amino-2-cyclobutyl-5-(6-methoxy-2-methylpyridin-3-yl)-2,3-dihydro-1H-pyrrolo[3,4-*b*]quinolin-1-one (**4**) and 9-amino-2-cyclobutyl-5-(2-methoxypyridin-3-yl)-2,3-dihydro-1H-pyrrolo[3,4-*b*]quinolin-1-one (**5**), were prepared as previously described.^{28,29} All other chemicals were obtained from commercial sources and were used as received without further purification unless indicated. For radiochemical syntheses, THF was freshly distilled under nitrogen from LiAlH₄. All water used was distilled and deionized (unless otherwise stated). A Scanditronix MC 17 cyclotron was used for radionuclide production. Purifications and analyses of radioactive mixtures were performed by HPLC with an in-line UV (254 nm) detector in series with a NaI crystal radioactivity detector (radiosynthesis and QC). Isolated radiochemical yields were determined with a dose calibrator (Capintec CRC-712M).

All animal experiments were carried out under humane conditions, with approval from the Animal Care Committee at the Centre for Addiction and Mental Health and in accordance with the guidelines set forth by the Canadian Council on Animal Care.

4.2. Chemistry

4.2.1. 9-Amino-2-cyclobutyl-5-(2-methyl-6-oxo-1,6-dihydropyridin-3-yl)-2,3-dihydro-1H-pyrrolo[3,4-*b*]quinolin-1-one (**7**)

A solution of 0.100 g (0.27 mmol) of 9-amino-2-cyclobutyl-5-(6-methoxy-2-methylpyridin-3-yl)-2,3-dihydro-1H-pyrrolo[3,4-*b*]quinolin-1-one (**4**) in 2 mL of toluene was stirred under N₂ as 0.167 g (0.53 mmol) of BBr₃·Me₂S complex was added. The mixture was heated at 100 °C for 2 h and was then cooled to room temperature. It was diluted with 4 mL of 1 N HCl and the resulting solid was removed by filtration. The solid was taken up in 80 mL of 30% MeOH in CH₂Cl₂ and the resulting slurry was sonicated and filtered to give **7** as an off-white solid (0.069 g, 72% yield): mp: 257–258 °C; ¹H NMR (400 MHz, MeOD/DMSO-*d*₆) δ (ppm) = 1.70–1.76 (m, 2H), 1.91 (s, 3H), 2.13–2.22 (m, 2H), 2.24–2.35 (m, 2H), 4.55–4.78 (m, 3H), 6.36 (d, $J = 8.4$ Hz, 1H), 7.31 (d, $J = 9.2$ Hz, 1H), 7.75 (t, $J = 7.9$ Hz, 1H), 7.83 (d, $J = 7.4$ Hz, 1H), 8.66 (d, $J = 8.6$ Hz, 1H). HRMS (ESI, positive mode) m/z , [$M+H$]⁺ calcd for C₂₁H₂₁N₄O₂⁺: 361.1659, found: 361.1629.

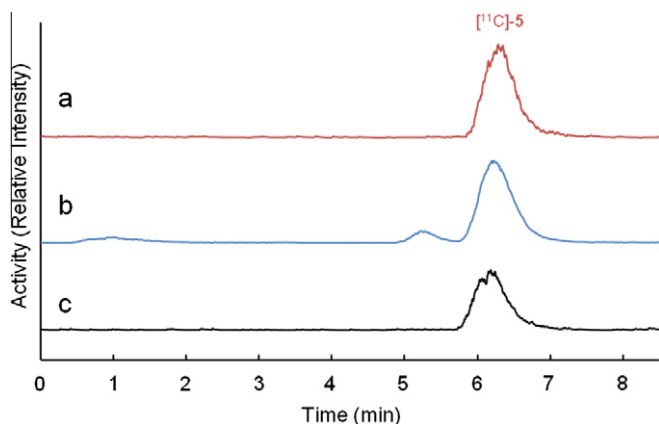


Figure 2. HPLC chromatograms of (a) rat brain extract after injection of [^{11}C]5 (15 min post injection), (b) rat plasma after injection of [^{11}C]5 (5 min post injection), and (c) control plasma containing [^{11}C]5. The peak at ca. 6.2 min corresponds to unmetabolized [^{11}C]5.

4.2.2. 9-Amino-2-cyclobutyl-5-(1,2-dimethyl-6-oxo-1,6-dihydropyridin-3-yl)-2,3-dihydro-1H-pyrrolo[3,4-b]quinolin-1-one (8)

A suspension of 0.131 g (0.36 mmol) of 9-amino-2-cyclobutyl-5-(2-methyl-6-oxo-1,6-dihydropyridin-3-yl)-2,3-dihydro-1H-pyrrolo[3,4-b]quinolin-1-one (**7**) in 4 mL of MeOH was stirred as 0.533 mL (0.80 mmol) of 1.5 M NaOH was added. After stirring the resulting solution for 10 min, 0.150 g (1.06 mmol) of iodomethane was added and the solution was stirred at room temperature overnight. The reaction mixture was diluted with 10 mL of 10% NaHCO₃ and the resulting solution was extracted three times with 10 mL of CH₂Cl₂. The combined organics were dried with MgSO₄ and then filtered, and the resulting solution concentrated to dryness. Purification by silica gel chromatography afforded **8** as an off-white solid (0.069 mg, 51%): mp: 235–236 °C; ¹H NMR (400 MHz, CDCl₃) δ (ppm) = 1.74–1.85 (m, 2H), 2.13 (s, 3H), 2.19–2.31 (m, 2H), 2.32–2.43 (m, 2H), 3.69 (s, 3H), 4.37–4.54 (m, 2H), 4.73–4.84 (m, 1H), 6.55 (d, J = 9.0 Hz, 1H), 7.40 (d, J = 9.2 Hz, 1H), 7.54 (dd, J = 7.1, 8.3 Hz, 1H), 7.60–7.65 (m, 1H), 8.26 (dd, J = 1.6, 8.4 Hz, 1H). HRMS (ESI, positive mode) m/z , $[M+H]^+$ calcd for C₂₂H₂₃N₄O₂⁺: 375.1816, found: 375.1788.

4.2.3. 9-Amino-2-cyclobutyl-5-(2-oxo-1,2-dihydropyridin-3-yl)-2,3-dihydro-1H-pyrrolo[3,4-b]quinolin-1-one (9)

A solution of 0.042 g (0.12 mmol) of 9-amino-2-cyclobutyl-5-(2-methoxypyridin-3-yl)-2,3-dihydro-1H-pyrrolo[3,4-b]quinolin-1-one (**5**) in 1 mL of toluene under nitrogen was stirred as 0.073 mg (0.23 mmol) of BBr₃·Me₂S complex was added and the resulting mixture was heated in at 100 °C for 3 h. After cooling to room temperature, 2 mL of aq 1 N HCl was added and the resulting precipitate was collected by filtration to afford of **9** as an off-white solid (0.040 g, 94%): mp: 242–243 °C; ¹H NMR (400 MHz, DMSO-*d*₆) δ (ppm) = 1.65–1.78 (m, 2H), 2.10–2.23 (m, 2H), 2.26–2.40 (m, 2H), 4.62–4.71 (m, 1H), 4.74 (s, 2H), 6.43 (t, J = 6.7 Hz, 1H), 7.65 (d, J = 6.8 Hz, 2H), 7.74 (dd, J = 7.4, 8.4 Hz, 1H), 7.84 (dd, J = 1.2, 7.2 Hz, 1H), 8.71 (dd, J = 1.4, 8.4 Hz, 1H), 8.8 (s, 1H), 9.95 (s, 1H), 12.09 (s, 1H). HRMS (ESI, positive mode) m/z , $[M+H]^+$ calcd for C₂₀H₁₉N₄O₂⁺: 347.1503, found: 347.1472.

4.2.4. 9-Amino-2-cyclobutyl-5-(1-methyl-2-oxo-1,2-dihydropyridin-3-yl)-2,3-dihydro-1H-pyrrolo[3,4-b]quinolin-1-one (10)

A suspension of 150 mg (0.35 mmol) of 9-amino-2-cyclobutyl-5-(2-oxo-1,2-dihydropyridin-3-yl)-2,3-dihydro-1H-pyrrolo[3,4-b]quinolin-1-one (**9**) hydrochloride in 3 mL of MeOH was stirred at room temperature as 0.517 mL (0.78 mmol) of aq 1.5 M NaOH was added. After 10 min, 150 mg (1.06 mmol) of iodomethane was added and the suspension was stirred at room temperature overnight. The solid was removed by filtration and was washed 2 × 10 mL water, 2 × 10 mL of ether, and 2 × 10 mL hexane. It was then purified by silica gel chromatography to give **10** as a white solid (0.125 g, 74%): mp: 187–188 °C; ¹H NMR (400 MHz, CDCl₃) δ (ppm) = 1.69–1.82 (m, 2H), 2.26 (m, 4H), 3.65 (s, 3H), 4.39 (s, 2H), 4.84 (m, 1H), 6.31 (t, J = 6.8 Hz, 1H), 6.68 (s, 2H), 7.17 (dd, J = 7.1, 8.3 Hz, 1H), 7.38 (dd, J = 2.0, 6.7 Hz, 1H), 7.48 (dd, J = 2.0, 6.8 Hz, 1H), 7.60 (dd, J = 1.5, 7.1 Hz, 1H), 7.70 (dd, J = 1.4, 8.4 Hz, 1H). HRMS (ESI, positive mode) m/z , $[M+H]^+$ calcd for C₂₁H₂₁N₄O₂⁺: 361.1659, found: 361.1628.

4.2.5. (R,S)-N-(1-(3-chloro-4-hydroxyphenyl)ethyl)-3,3-diphenylpropan-1-amine (11)

To 0.14 g (0.37 mmol) of (R,S)-N-(1-(3-chloro-4-methoxyphenyl)ethyl)-3,3-diphenylpropan-1-amine (**6**) was added 2 mL of a 48% HBr solution in acetic acid and 4 mL of glacial acetic acid. The mixture was heated to 120 °C and stirred for 24 h. The solution was evaporated under vacuum and the crude product was redissolved in 7 mL of CHCl₃, and the organic phase was washed with

a 1 M NaHCO₃ solution. The aqueous phase was back-extracted with a 1:5 mixture of MeOH/CHCl₃ (6 mL) and the combined organic extracts were dried (MgSO₄), filtered and concentrated under vacuum. The product was purified by preparative TLC (10:1 CHCl₃/MeOH) to give 71 mg of **11** (52%) as an off-white solid: mp: 62 °C (free base); ¹H NMR (400 MHz, CDCl₃) δ (ppm) = 1.29 (d, J = 6.65 Hz, 3H), 2.14–2.36 (m, 2H), 2.39–2.58 (m, 2H), 3.63 (q, J = 6.65 Hz, 1H), 3.96 (t, J = 7.83 Hz, 1H), 6.85 (d, J = 8.22 Hz, 1H), 7.01 (dd, J = 1.96, 8.22 Hz, 1H), 7.11–7.33 (m, 11H). HRMS (ESI, positive mode) m/z , $[M+H]^+$ calcd for C₂₃H₂₅NOCl⁺: 366.1619, found: 366.1603.

4.3. Radiosynthesis of [¹¹C]**4** and [¹¹C]**5**

The method of Crouzel,⁴⁶ with some modifications, was used to produce [¹¹C]CH₃I. Preparation of the carbon-11 labelled compounds was accomplished via the 'LOOP' method³⁸ using a modified radiosynthesis module as previously described.³⁹ Precursors **7** (0.25 mg, 0.69 μ mol) and **9** (0.25 mg, 0.72 μ mol) were dissolved in 80 μ L of DMF and DMSO, respectively. The solution of **7** (**9**) was added to a vial filled with 6 mg (18.4 μ mol) of Cs₂CO₃ and vortexed for 3 min. The resulting bright yellow solution was then decanted from the excess solid carbonate via syringe and injected into a clean, dry loop.³⁸ The [¹¹C]CH₃I was then introduced, and the mixture was reacted for 1 minute at ambient temperature. The reaction mixture was then purified via HPLC (LUNA C18(2), 250 × 10 mm, 10 μ ; 60:40 CH₃CN/H₂O + 0.1 N NH₄⁺HCO₂[−]; 5 mL/min (3 mL/min), 254 nm; Figs. S1a and S2a). The radiochemical peak (7.3 min, [¹¹C]**4**; 9.2 min, [¹¹C]**5**) was collected and formulated as previously described.⁴⁷ The formulated product was analyzed by HPLC (Prodigy C18 ODS3 (250 × 4.6 mm, 10 μ ; 60:40 CH₃CN/H₂O + 0.1 N NH₄⁺HCO₂[−]; 2 mL/min (1.5 mL/min), 254 nm) with a retention time of 3.6 min (3.9 min; Figs. S1b and S2b). The radiochemical yield (2.9%, 910.6 MBq, 24.6 mCi, [¹¹C]**4**; 2.7%, 847.8 MBq, 23.0 mCi, [¹¹C]**5**), uncorrected for decay (based on our full scale production of [¹¹C]CO₂ (31.4 GBq; 850 mCi), had specific activities of 100 ± 30 GBq μ mol^{−1} (2.7 ± 0.9 Ci μ mol^{−1}; n = 6) and 70 ± 20 GBq μ mol^{−1} (2.0 ± 0.5 Ci μ mol^{−1}; n = 6), respectively, with radiochemical purities >95%.

4.4. Radiosynthesis of [¹¹C]**6**

The desmethyl precursor, **11** (1.4 mg, 3.8 μ mol), was dissolved (with vigorous vortexing for ca. 2 min) in a mixture of 72.5 μ L of DMF and 3.5 μ L of 1 N TBAOH (3.5 μ mol, in MeOH), followed by loading onto the HPLC loop. After a 5-min reaction with [¹¹C]CH₃I, the product was purified using a Phenomenex Luna (2) C18 10 μ (250 × 10 mm) column and 60:40 CH₃CN/H₂O + 0.1 N NH₄HCO₂ as the mobile phase with a flow rate of 5.0 mL min^{−1} (λ = 254 nm; Fig. S3). The [¹¹C]CH₃I reacted with **11** to form [¹¹C]**6** (81% conversion by HPLC, t_R ≈ 9 min) and was well separated during purification. Purified [¹¹C]**6** was formulated in 10% EtOH/saline as described previously.³⁹ At the end of synthesis (30 min) the final product contained 4.9 GBq (133 mCi) starting [¹¹C]CO₂: 31.4 GBq, 850 mCi. The radiochemical purity was determined by analytical HPLC using a Phenomenex Luna C18 10 μ (250 × 4.6 mm) column using a flow rate of 2.0 mL min^{−1} and eluted with 60:40 CH₃CN/H₂O + 0.1 N NH₄HCO₂ (λ = 280 nm; Fig. S4). Co-injections of [¹¹C]**6** with authentic **6** were performed under several other HPLC conditions (columns, wavelengths, mobile phases) to confirm radiochemical purity. The radiochemical yield of [¹¹C]**6** was 16% (5.0 GBq, 136 mCi); uncorrected for decay, based on production of 31.4 GBq (850 mCi) of [¹¹C]CO₂, with a specific activity of 160 ± 40 GBq μ mol^{−1} (4.3 ± 1.2 Ci μ mol^{−1}; n = 3) and radiochemical purity >99% at end of synthesis.

4.5. Ex vivo biodistribution

Preliminary ex vivo biodistribution studies of [^{11}C]4, [^{11}C]5, and [^{11}C]6 in conscious male Sprague-Dawley rats were conducted ($n = 1$ rat per time point) as previously described.^{40,48} For the full biodistribution study, all rats received ca. 37 MBq (1 mCi) of [^{11}C]5 in 0.3 mL of buffered saline (containing 10% ethanol) via the tail vein and were sacrificed by decapitation at either 5, 15, 30 or 60 min after injection ($n = 4$ per time point). The brains were removed, and regions of interest were excised, blotted, weighed and then counted for radioactivity (Table 1).

4.6. Blocking studies

Rats received intraperitoneal injections of a solution (0.4–0.6 mL) of 5% DMSO/5% EtOH in saline (containing 5% Tween80 w/w; vehicle), 0.1 mg/kg of 5, 5 mg/kg of 5, or 10 mg/kg of flumazenil at 30 min before administration of [^{11}C]5. Using the protocol described above, rats were sacrificed and dissected at 15 min post-injection of the radiotracer (Table 2).

4.7. Metabolism studies

Following tail-vein injection of [^{11}C]5, as described above, whole blood was collected at 5 and 15 min from the trunk in a heparinized tube and centrifuged. The plasma was analyzed by radio-HPLC using the method of Hilton and coworkers,⁴⁹ with minor modifications.⁵⁰ Briefly, rat plasma from either time point was directly loaded onto a 5 mL HPLC injector loop and injected onto a capture column (4.6 mm \times 20 m) that was packed in-house with OASIS HLB 30 μm (Waters, NJ). The capture column was eluted with 1% aqueous CH_3CN (2 mL/min) for approximately 3 min and then back-flushed with 50:50 $\text{CH}_3\text{CN}/\text{H}_2\text{O} + 0.1 \text{ N NH}_4^+\text{HCO}_3^-$ (pH 4); 2.0 mL/min onto a Phenomenex Luna C18 Column (250 \times 4.6 mm, 10 μm). The column effluents from both columns were monitored through a flow detector (Bioscan Flow-Count) operated in coincidence mode. Whole brain from a control rat was removed and treated with ca. 1.3 MBq (37 μCi) of [^{11}C]5, and the whole brain was removed from rats sacrificed at 5 or 15 min post-injection. Brains were individually homogenized with ice-cold 80:20 $\text{CH}_3\text{CN}/\text{H}_2\text{O} + 0.01 \text{ N HCl}$ and centrifuged as previously described by our laboratory,⁵⁰ prior to radio-HPLC analysis of the supernatant using the aforementioned method.

Acknowledgements

The authors thank Armando Garcia, Winston Stableford and Min Wong for assistance with the radiochemistry, and Justin Hicks for assistance with the log $D_{7.4}$ determinations. CAMH is gratefully acknowledged for support in the form of a post-doctoral fellowship (M.D.M.).

Supplementary data

Supplementary data associated with this article can be found, in the online version, at <http://dx.doi.org/10.1016/j.bmc.2012.05.046>.

References and notes

- Nutt, D. J.; Malizia, A. L. *Br. J. Psychiatry* **2001**, 179, 390.
- Mehta, A. K.; Ticku, M. K. *Brain Res. Rev.* **1999**, 29, 196.
- Jakobsen, S.; Kodahl, G. M.; Olsen, A. K.; Cumming, P. *Nucl. Med. Biol.* **2006**, 33, 593.
- Rudolph, U.; Möhler, H. *Annu. Rev. Pharmacol. Toxicol.* **2004**, 44, 475.
- Krystal, J. H.; Staley, J.; Mason, G.; Petrakis, I. L.; Kaufman, J.; Harris, R. A.; Gelernter, J.; Lappalainen, J. *Arch. Gen. Psychiatry* **2006**, 63, 957.

- Katsifis, A.; Kassiou, M. *Mini-Rev. Med. Chem.* **2004**, 4, 909.
- Sieghart, W. *J. Psychiatr. Neurosci.* **1994**, 19, 24.
- Sieghart, W. *Pharmacol. Rev.* **1995**, 47, 181.
- Korpi, E. R.; Matilla, M. J.; Wisden, W.; Luddens, H. *Ann. Med.* **1997**, 29, 275.
- Atack, J. R. *Curr. Drug Targets CNS Neurol. Disord.* **2003**, 2, 213.
- Maziere, M.; Hantraye, P.; Prenant, C. H.; Sastre, J.; Comar, D. *Int. J. Appl. Radiat. Isot.* **1984**, 35, 973.
- Hammers, A. *Neuroimag. Clin. N. Am.* **2004**, 14, 537.
- Halldin, C.; Stone-Elender, S.; Thorell, J.-O.; Persson, A.; Sedvall, G. *J. Radiat. Appl. Instrum. Part A* **1988**, 39, 993.
- Ryzhikov, N. N.; Seneca, N.; Krasikova, R. N.; Gomzina, N. A.; Shchukin, E.; Fedorova, O. S.; Vassiliev, D.; Gulyás, B.; Hall, H.; Savic, I.; Halldin, C. *Nucl. Med. Biol.* **2005**, 32, 109.
- Odano, I.; Halldin, C.; Karlsson, P.; Varrone, A.; Airaksinen, A. J.; Krasikova, R. N.; Farde, L. *NeuroImage* **2009**, 45, 891.
- Beer, H. F.; Blauenstein, P. A.; Hasler, P. H.; Delaloye, B.; Ricabona, G.; Bangerl, I.; Hunkeler, W.; Bonetti, E. P.; Piere, L.; Richards, J. G. *J. Nucl. Med.* **1990**, 31, 1007.
- Westera, G.; Buck, A.; Burger, C.; Leenders, K. L.; von Schulthess, G. K.; Schubinger, A. P. *Eur. J. Nucl. Med.* **1996**, 23, 5.
- Halldin, C.; Farde, L.; Litton, J.-E.; Hall, H.; Sedvall, G. *Psychopharmacology* **1992**, 108, 16.
- Lingford-Hughes, A.; Hume, S. P.; Feeney, A.; Hirani, E.; Osman, S.; Cunningham, V. J.; Pike, V. W.; Brooks, D. J.; Nutt, D. J. *J. Cereb. Blood Flow Metab.* **2002**, 22, 878.
- Maeda, J.; Suhara, T.; Kawabe, K.; Okauchi, T.; Obayashi, S.; Hojo, J.; Suzuki, K. *Synapse* **2003**, 47, 200.
- Coenen, H. H.; Moerlein, S. M. *J. Fluorine Chem.* **1987**, 36, 63.
- Grunder, G.; Siessmeier, T.; Lange-Asschenfeldt, C.; Vernaleken, I.; Buchholz, G. G.; Stoeter, P.; Drzezga, A.; Luddens, H.; Rösch, F.; Bartenstein, P. *Eur. J. Nucl. Med.* **2001**, 28, 1463.
- Todde, S.; Moresco, R. M.; Fröstl, W.; Stampf, P.; Matarrese, M.; Carpinelli, A.; Magni, F.; Kienle, M. G.; Fazio, F. *Nucl. Med. Biol.* **2000**, 27, 565.
- Prenant, C.; Crouzel, C.; Valois, J. M.; Robertson, D. W.; Comar, D. *Appl. Radiat. Isot. Int. J. Radiat. Appl. Instrum. Part A* **1992**, 43, 946–948.
- Maziere, M.; Godot, J.-M.; Berger, G.; Prenant, C. H.; Comar, D. *J. Radioanal. Chem.* **1980**, 56, 229.
- Ishiwata, K.; Yanai, K.; Ido, T.; Miura-Kanno, Y.; Kawashima, K. *J. Radiat. Appl. Instrum. Part B* **1988**, 15, 365.
- Johnströma, P.; Stone-Elender, S.; Buelfer, T. *J. Labelled Compd. Radiopharm.* **1994**, 34, 147.
- Alhambra, C.; Becker, C.; Blake, T.; Chang, A.; Damewood, J. R. J.; Daniels, T.; Dembofsky, B. T.; Gurley, D. A.; Hall, J. E.; Herzog, K. J.; Horchler, C. L.; Ohnmacht, C. J.; Schmiesing, R. J.; Dudley, A.; Ribadeneira, M. D.; Knappenberger, K. S.; Maciag, C.; Stein, M. M.; Chopra, M.; Liu, X. F.; Christian, E. P.; Arriza, J. L.; Chapdelaine, M. J. *Bioorg. Med. Chem.* **2011**, 19, 2927.
- Chang, H.-F.; Chapdelaine, M. J.; Dembofsky, B. T.; Herzog, K. J.; Horchler, C.; Schmiesing, R. J. *WO Patent 2008/155572 A2*.
- Orrü, A.; Lai, P.; Lobina, C.; Maccioni, P.; Piras, P.; Scanu, L.; Froestl, W.; Gessa, G. L.; Carai, M. A. M.; Colombo, G. *Eur. J. Pharmacol.* **2005**, 525, 105.
- Liang, J.-H.; Chen, F.; Krstew, E.; Cowen, M. S.; Carroll, F. Y.; Crawford, D.; Beart, P. M.; Lawrence, A. J. *Neuropharmacology* **2006**, 50, 632.
- Slattery, D. A.; Markou, A.; Froest, W.; Cryan, J. F. *Neuropsychopharmacology* **2005**, 30, 2065.
- Tsai, M.-L.; Shen, B.; Leung, L. S. *Epilepsy Res.* **2008**, 79, 187.
- Kato, K.; Zhang, M.-R.; Suzuki, K. *Bioorg. Med. Chem. Lett.* **2009**, 19, 6222.
- Kerr, D. I. B.; Ong, J.; Perkins, M. V.; Prager, R. H.; Puspawati, N. M. *Aust. J. Chem.* **2006**, 59, 445.
- Hopkins, G. C.; Jonak, J. P.; Minnemeyer, H. J.; Tieckelmann, H. J. *Org. Chem.* **1967**, 32, 4040.
- Singh, B. K.; Cavalluzzo, C.; Maeyer, M. D.; Debyser, Z.; Parmar, V. S.; Eycken, E. V. D. *Synthesis* **2009**, 8, 2725.
- Wilson, A. A.; Garcia, A.; Jin, L.; Houle, S. *Nucl. Med. Biol.* **2000**, 27, 529.
- Wilson, A. A.; Garcia, A.; Houle, S.; Vasdev, N. J. *Labelled Compd. Radiopharm.* **2009**, 52, 490.
- Vasdev, N.; Natesan, S.; Galineau, L.; Garcia, A.; Stableford, W. T.; McCormick, P.; Seeman, P.; Houle, S.; Wilson, A. A. *Synapse* **2006**, 60, 314.
- Wong, D. F.; Pomper, M. G. *Mol. Imag. Biol.* **2003**, 5, 350.
- Waterhouse, R. N. *Mol. Imaging Biol.* **2003**, 5, 376.
- Wilson, A. A.; Jin, L.; Garcia, A.; DaSilva, J. N.; Houle, S. *Appl. Radiat. Isot.* **2001**, 54, 203.
- Pirker, S.; Schwarzer, C.; Wieselthaler, A.; Sieghart, W.; Sperk, G. *Neuroscience* **2000**, 101, 815.
- Pike, V. W. *Trends Pharmacol. Sci.* **2009**, 30, 431.
- Crouzel, C.; Långström, B.; Pike, V. W.; Coenen, H. H. *Appl. Radiat. Isot. Int. J. Radiat. Appl. Instrum. Part A* **1987**, 38, 601.
- van Oosten, E. M.; Wilson, A. A.; Stephenson, K. A.; Mamo, D. C.; Pollock, B. G.; Mulsant, B. H.; Yudin, A. K.; Houle, S.; Vasdev, N. *Appl. Radiat. Isot.* **2009**, 67, 611.
- Wilson, A. A.; DaSilva, J. N.; Houle, S. *Nucl. Med. Biol.* **1996**, 23, 141.
- Hilton, J.; Yokoi, F.; Dannels, R. F.; Ravert, H. T.; Szabo, Z.; Wong, D. F. *Nucl. Med. Biol.* **2000**, 27, 627.
- Wilson, A. A.; Garcia, A.; Parkes, J.; McCormick, P.; Stephenson, K. A.; Houle, S.; Vasdev, N. *Nucl. Med. Biol.* **2008**, 35, 305.